

**Material Properties and Temperature Effects Quantified for Slurry Wear –
16141**

Consuelo Guzman-Leong
LPI, Inc.
cguzman-leong@lpiny.com

Joseph Cluever
LPI, Inc.
jcluever@lpiny.com

Steve Gosselin
LPI, Inc.
sgosselin@lpiny.com

ABSTRACT

Literature indicates that the hardness of solid particles relative to the target material hardness and temperature influence erosion. Investigations of temperature effects on erosion also show that erosion resistance is a function of target material's homologous temperature to melting point temperature. While relative hardness effects on erosion and temperature effects on erosion have been investigated independently, their combined effect has not been evaluated. This paper summarizes a review of relevant literature on relative hardness and temperature effects on erosion and via probabilistic calculations, quantifies the combined effect of relative hardness and temperature on liquid-particle induced wear, or slurry wear. These insights can assist material selection and plant operations at waste processing facilities.

INTRODUCTION

Transporting liquid-particle slurries is a major industrial process. Slurry-induced wear is of significant importance in determining the service life of the major components handling liquids with hard abrasives in waste and chemical handling equipment, exposed parts in marine environments, turbine blades of hydro-electric power plants, mineral processing and mining systems to name a few [Chawla et al. 2013]. A total degradation loss model caused by flowing liquid-particle slurries was developed to predict component reliability over time. This model can be used to quantify relative hardness and temperature effects over a range of particle hardness and temperatures. The slurry wear model for piping components calculates the total wear rate from the superposition of the major parameters including erosion, general corrosion, and the synergy between erosion and general corrosion. By classifying each of the major parameters it is possible to predict component total degradation and failure life time using distributions of parameters and statistical methods.

MODELS

Erosion-Corrosion

Total wear is modeled as the sum of pure erosion, pure corrosion, and the synergy between erosion and corrosion. Erosion-corrosion synergy is the amount of total wear that cannot be accounted for by considering pure erosion and pure corrosion by

themselves. To account for wear in fittings and bends, the total wear (meters per second, mps) is scaled by a geometry factor G . This relationship is given in Equation 1.

$$T = (E + Q + S)G \quad \text{Eq. 1}$$

Where,

- T - Total wear (mps)
- E - Erosion rate (mps)
- Q - Corrosion rate (mps)
- S - Synergy wear rate (mps)
- G - Geometry factor

Erosion, corrosion, and synergy are individually modeled and described later. For probabilistic analysis, all of the stressors (particle size, pH, velocity, etc.) are independently sampled from their respective distributions. In addition to the aleatory uncertainty in the stressors, the epistemic uncertainty in the synergy wear rate and the parameters corresponding to the dominant stressors in the erosion-only model is also considered.

Erosion Only

Pure erosion is modeled as having a power law relationship with three dominant stressors and proportional to four additional factors. The dominant factors are slurry velocity, mass fraction of particle concentration, and average particle size. The less significant factors are the ratio of particle hardness (Vicker's) to target hardness (Vicker's) [Desale et al. 2008], the homologous temperature of the target material (ratio of absolute temperature to absolute melting temperature), and the shape of the particle. This relationship is given in Equation 2. The model parameters can be obtained from test data. The current effort considered stainless steel test data to obtain values for the model parameters.

$$E = e^k V^r \bar{P}^s C^t F_{hard} F_{temp} F_{shape} \quad \text{Eq. 2}$$

Where,

- E - Erosion rate (mps)
- V - Velocity (m/s)
- \bar{P} - Mean particle size (microns)
- C - Solids concentration (mass fraction)
- F_{hard} - Hardness factor
 $= \tanh\left(0.06477 \frac{\text{particle hardness (Vicker's)}}{\text{target hardness (Vicker's)}}\right)$

F_{temp} - Temperature factor
 $= \exp(2.9394T_{Hom})$

F_{shape} - Shape factor
 $= 1.9911 \times SPQ + 0.5584$

k, r, s, t - Model parameters (follow a multivariate normal distribution)

Corrosion Only

Pure corrosion is modeled as a reference corrosion rate adjusted by pH, temperature, and velocity factors. This relationship is shown in Equation 3.

$$Q = U_{ref} H R F_{vel} \quad \text{Eq. 3}$$

Where,

Q - Corrosion rate (mps)

U_{ref} - Uniform corrosion reference rate (mps)

H - pH factor

$$H \approx \begin{cases} \exp\left[\left(\frac{pH}{4.8}\right)^{-1.05937} - 1\right], & 0.8 < pH \leq 4.8 \\ 1, & 4.8 < pH \leq 9.2 \\ \exp\left[-5.7233 \ln^2\left(\frac{pH}{9.2}\right) - 1.2703 \ln\left(\frac{pH}{9.2}\right)\right], & 9.2 < pH \leq 14.2 \end{cases}$$

R - Temperature factor

F_{vel} - Velocity factor
 $= 1 + 0.140 \times V$

The pH factor was determined by plotting multiple sets of relative corrosion rates for corrosion tests that only varied the pH. A line was hand drawn between the data points and curves were fit to the various hand drawn segments. The velocity factor was calculated by comparing multiple sets of corrosion data that only varied the velocity of the fluid.

Synergy

The synergy model is dependent upon the erosion rate, corrosion rate, pH, fluid velocity, and whether the metal is stainless steel or a nickel-based alloy. For simulation purposes, a lognormally distributed multiplicative error term is included to account for uncertainty in the model's ability to make predictions. The synergy model is given in Equation 4. The model parameters can be obtained from test data. The

current effort considered stainless steel test data to obtain values for the model parameters.

$$S = b \cdot E^c Q^d x^{pH} V^y z^{I_{Nickel}} S_{error} \quad \text{Eq. 4}$$

Where,

- S - Synergy rate (mps)
- E - Erosion rate (mps)
- Q - Corrosion rate (mps)
- pH = $-\log_{10}$ (hydrogen concentration)

- V - Velocity (m/s)
- I_{Nickel} = $\begin{cases} 0, & \text{if material is stainless steel} \\ 1, & \text{if material is a nickel based alloy} \end{cases}$
- S_{error} - Random synergy error term (lognormally distributed)
- b, c, d, x, y, z - Model parameters

MATERIAL PROPERTIES

Materials selected for process vessels match the requirements for strength, corrosion resistance, fabricability, cost, availability, and other properties. Design codes define materials by their alloy chemistry (UNS number) and their properties. Often, knowledge of the product form and compositions can provide the user with a reasonable understanding of the material properties, however abrasive erosion resistance is not strictly based on strength or chemical composition. Typically, hardness of the material and the hardness of the abrasive are important indicators of the kinds of damage that is possible. Table I shows material properties for some stainless steel and nickel-based materials. Even though the nickel alloys have improved strength over the austenitic stainless steels, it is not necessarily reflected in higher hardness for the wrought alloys.

Table I. Alloy Chemistry and Material Properties of Common Materials

Specification		Major Chemical Constituents								Minimum Mechanical Properties			
Trade Name	UNS Number	Fe	C	Ni	Cr	Mo	W	Co	Cu	UTS	Yield	Rockwell	Vickers Hv
										KSI	KSI	R _B	
Type 304L	S30403	bal	0.03	8-12	18-20	-	-	-	-	70	25	82	156
Type 316L	S31603	bal	0.03	16-18	16-18	2-3	-	-	-	70	25	79	147
6% Mo	N08637	bal	0.03	23-25	20-22	6-7	-	-	0.75	110	55	90	186
Inconel 690	N06690	7-11	0.05	bal	27-31	-	-	-	0.5	110	66	85	165
Alloy C-22	N06022	2-6	0.01	bal	20-22	12-14	2-3	2.5	-	100	45	89-93	180-200
Alloy C-276	N10276	4-7	0.01	bal	14-16	15-17	3-4	2.5	-	100	41	88-92	176-195

*ASTM E 140 Conversions

Material Hardness

Erosion–corrosion is a complex material degradation mechanism involving mechanical erosion and electrochemical corrosion. For components in waste or mineral processing plants, erosion-corrosion wear (wall thinning) is associated with the transport of liquids containing slurry particles. The literature indicates that the hardness of the abrasive and target materials are important parameters for estimating erosion-corrosion. Flinn and Trojan (1995) define hardness of a material as its resistance to penetration and plastic deformation. Hardness is an intrinsic material property that is influenced by several factors including crystal structure, fabrication methods, chemical composition, and microstructure [ASM 1992]. There are several tests available to quantify a materials hardness, but the Vickers hardness test is better for obtaining hardness measurements at high levels and for measuring the hardness of a small region [Flinn and Trojan 1995]. The Vickers hardness test uses a diamond pyramid for impression into a material. The Vickers hardness (Hv) is associated with the measured diagonal of the square impression on the material.

Target material wear generally occurs when the abrasive hardness exceeds the target material hardness. Even when the abrasive itself is deformed in the process, it is still capable of removing material [ASM 1992]. The level of wear depends on the relative hardness (*RH*), or the ratio of abrasive hardness and target material hardness [Fisher and Bobzin 2009]. Fisher and Bobzin (2009) indicate that the target material experiences negligible wear when the hardness of the abrasive is low relative to its hardness. When the abrasive particle is of comparable hardness to the wear material, the momentum transferred from the particle causes elastic and plastic deformation in the form of small craters, disturbed metal, and micro-fractures. Higher levels of wear occur when the hardness of the abrasive is much greater than the target

material hardness. When $RH \gg 1$, the abrasive is able to penetrate the target material's surface and cut/remove material without having its cutting edges broken or rounded [ASM 1992]. Plastic deformation is more pronounced when the abrasive particle is harder than the target material and the particle collides with the surface, forming a wedge or crater causing small micro-fractures.

Investigations by Clark and Llewellyn (2001) and Desale et al. (2008) reveal that the hardness of solid particles relative to the target material hardness influences erosive wear. Clark and Llewellyn provided slurry erosion data across 11 wear resistant plates and pipeline steels (Vickers hardness less than ~ 750 HV), and two apparatuses. One of the two hardness test apparatus involved the Coriolis erosion tester. The Coriolis tester method is designed to simulate aqueous slurry-induced wear in slurry pumps and cyclones, and consists of a rotor with a diametral passage (holds specimens). Target materials were tested in tap water (pH=7 and $Cl^- < 1.5$ ppm) containing 10 wt% silica sand particles (212-300 microns, 750 HV, density of 2650 kg/m^3). Clark and Llewellyn graphed the relationship between steel (Vickers) hardness and relative erosion resistance (volume of material loss relative to AISI 1020, 139 HV), as shown in Fig. 1. Desale et al. performed slurry pot tests to investigate the hardness ratio (erodent hardness and target material hardness) effects on the erosion rate at normal impact conditions. Seven different target materials were considered, including Type 304L and Type 316L stainless steels. Experiments were performed at 3 m/s velocity, and 10 wt% concentration of 550 microns particles of quartz, alumina, and silicon carbide.

Consistent with Fisher and Bobzin (2009), a hyperbolic tangent function was used to correlate relative wear rates reported by Clark and Llewellyn (2001) and Desale et al. (2008) to the ratio of solid particle to target material Vickers hardness (Hv). The hardness factor defines the correlation between relative wear and relative hardness (RH) as shown in Fig. 1. An average hardness factor of ~ 0.09 represents an average particle hardness of $HV = 255$ and an average target material hardness of $HV = 193$.

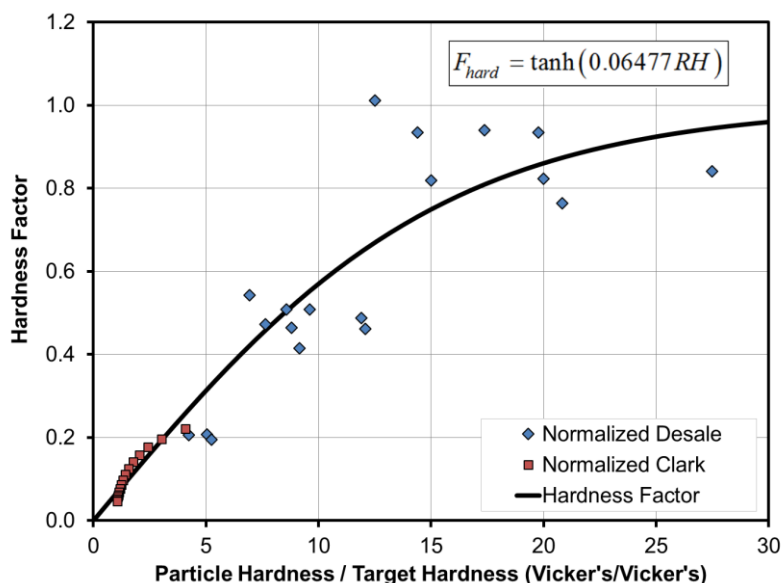


Fig. 1. Hardness Adjustment Factor (Erosion)

Particle Shape

Particle shape also influences erosion wear of the abrasive as the shape of the impacting particle influences the shape of the groove produced in the target material [ASM 1992]. Particles with sharp and fractured edges cut trenches in the surface whereas rounded particles indent, crater and plow grooves the surface. Particle shape refers to the degree or deviation of sphericity. The severity of wear varies depending on the combination of the ductile or brittle nature of the target material, roundness or sharpness of the impacting particle as well as the relative hardness of the target material to the particle hardness.

Different expressions for quantifying particle shape are reported in the literature. The statistical parameter R_{ku} for describing a particle's edge detail [Stachowiak 2000], particle aspect ratio (W/L) and the P^2/A quotient have been used to quantify particle shape, where perimeter (P), area (A), and W and L are the minimum distances between two parallel planes [Badahur and Badruddin 1990]. Deviations of P^2/A from 4π indicate departure from sphericity. Particle shape characterization is achieved by performing photo imaging via scanning electron microscopes and subsequent analysis via software or manual inspection.

Particle shape has also been quantified by a spike parameter quadratic (SPQ). SPQ is a weighted-average of spike angles of a solid particle. Fig. 2 illustrates how the spike angles are measured as the intersecting angle between parabolas fit to the perimeter of the particle image that extends beyond the average radius. As shown in Fig. 2, a spherical particle has an SPQ value of 0, where a particle with many "spikes" has an SPQ value of unity. Clearly, a particle with an SPQ approaching unity

will cause more damage than if the particle was perfectly rounded ($SPQ \approx 0$) because of its ability to penetrate the target material surface. Similarly, Bahadur and Badruddin (1990) showed that erosion increases with increasing P^2/A and decreasing aspect ratio (W/L).

Experiments have confirmed that less wear occurs when the target material is worn by rounded, rather than sharp particles [Bahadur and Badruddin 1990, Stachowiak 2000]. Stachowiak (2000) measured the particle shape in terms of SPQ for various particles including glass beads, silica sand, silicon carbide and quartz, as shown in Table II.

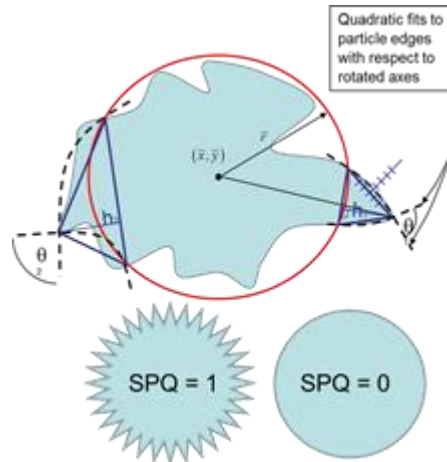


Fig. 2. Spike Value Quadratic

Table II. SPQ for Three Solids used for Testing the Influence of Particle Shape [Stachowiak 2000]

Abrasive	SPQ
Glass Beads	0.0231
Silica Sand	0.1919
Silicon Carbide	0.4247

Stachowiak measured average erosive wear in air (glass target material) at various impact angles and particle types (250-300 microns). The shape factor is based on the average wear versus particle impact angle data presented in Stachowiak (2000) for various particles (having different hardness and SPQ 's). Non-linear regression was employed to obtain the correlation between particle shape (SPQ) and erosive wear – independent of particle impact angle and particle hardness. Fig. 3 illustrates the change in erosive wear as a function of particle shape (SPQ). Probabilistic modeling simulations sample on the particle SPQ , and the erosion rate is adjusted accordingly. A silica sand particle with an SPQ of 0.1919 results in an average particle shape factor of ~ 0.94 .

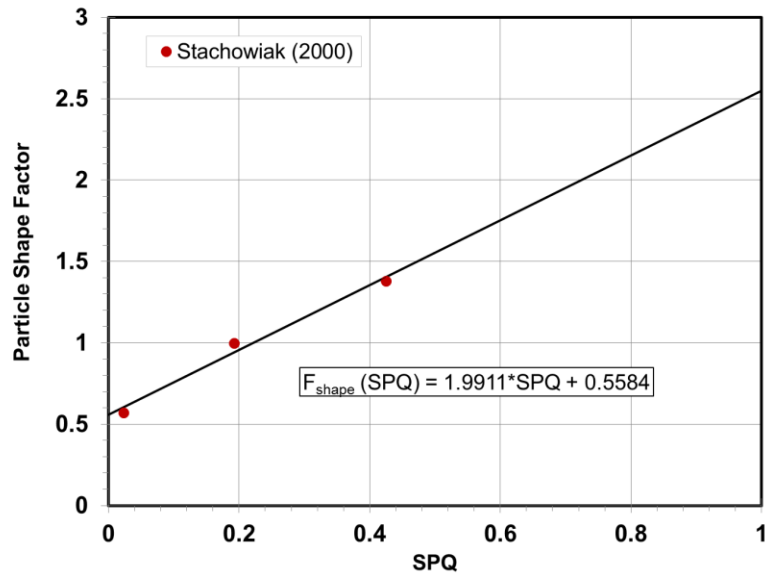


Fig. 3. Particle Shape Factor (Erosion)

General Corrosion Rate

General corrosion refers to uniform anodic dissolution wall thinning of a material due to the electrochemical interaction between the material and its environment. Consequently, a material’s corrosion rate depends on its exposed environment (i.e., corrosion from exposure to distilled water versus corrosion from exposure to hydrochloric acid). The probabilistic erosion-corrosion model uses an average uniform corrosion rate of $U_{ref} = 1.61E-14$ mps for austenitic stainless steels. The nickel-based alloys calculations use a uniform (reference) corrosion rate of $U_{ref} = 4.83E-16$ mps. These reference corrosion rates are at zero velocity, a reference pH of 7 and a temperature of $\sim 21^\circ\text{C}$.

Temperature Effects

Erosion-corrosion is a degradation mechanism comprised of mechanical and electrochemical wear contributions. Temperature effects on chemical processes is well established and quantified by the Arrhenius relationship, shown in Equation 5. The corrosion term shown in Equation 5 is modified to account for changes in temperature relative to a reference corrosion rate. The uniform corrosion rate is adjusted by the temperature R factor, based on the ratio of (sampled) process temperature and room temperature. An average activation energy value of 30 kJ/mol that is consistent for Type 316L stainless steel is also used [Refaey et al. 2006]. An average temperature adjustment factor for uniform corrosion of $R \sim 2.5$ represents an operating temperature of 45°C (318 K).

$$R = e^{(A_r/Rg)(1/T_{ref} - 1/T)} \tag{Eq. 5}$$

Where,

R	- Temperature adjustment factor
A_r	- Activation Energy (J/mol)
R_g	- Gas Constant (8.31434 J/mol/K)
T_{ref}	- Reference Temperature (294 K)
T	- Sampled operating Temperature (K)

Unlike temperature effects on chemical processes, it is important to isolate direct versus secondary temperature effects on mechanically-induced (erosion-only) wear. Duignan and Lee (2001) describe experiments where the increase in wear associated with temperature changes was actually driven by secondary effects like stress corrosion cracking for slurries including chlorides and fluorides, and change in slurry viscosity. Investigations attempting to quantify temperature effects on mechanically-induced wear should avoid conditions that introduce unintentionally electrochemical processes (i.e., avoid moisture in test environment).

Gat and Tabakoff (1980) provided erosion resistance data for Type 304 stainless steel. Erosion resistance data was shown to be a function of homologous temperature T_{Hom} , ratio of operating temperature (K) to melting point temperature (K). Test conditions were for a flow of air with entrained quartz particles, and 86 μm (microns) ash particles, at various impact angles (15, 25, 45, 60, 75, and 90-degrees) and velocities (152, 183, 244, 305 m/s) for temperatures between 5 °C and 210 °C. Consistent with temperature effect versus wear resistance discussions in ASM (1992) and Flinn and Trojan (1995), Gat and Tabakoff (1980) showed that as temperature increases, the metals' resistance to erosion decreases.

Fig. 4 shows the temperature factor based on the Gat and Tabakoff test data. The second horizontal scale in Fig. 4 indicates the operating temperature in degrees Fahrenheit based on the Type 304 SS melting point temperature (average of 1427.5 °C) reported by Gat and Tabakoff (1980). Based on a slurry temperature of 90°C and an average melting point temperature of 1425°C for Type 304L stainless steel materials, the average temperature factor is 1.87. For perspective, Hastelloy C-276 melts at ~1325 °C, resulting in an average temperature factor of 1.95.

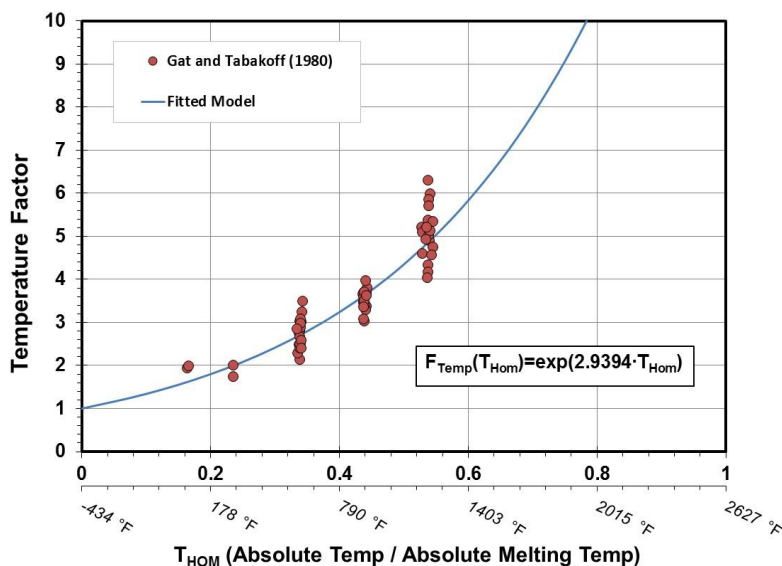


Fig. 4. Temperature Adjustment Factor (Erosion)

TEST CASES

Sensitivity studies were performed for nickel based alloy and austenitic stainless steel straight pipes using the probabilistic erosion-corrosion model described herein. The objectives of the studies were to determine the best-estimate probability of exceeding a wear allowance at 40 years and the average wear rate over the 40 years for several conditions. Two temperatures, two particle hardness, and two particle shapes were considered in the studies for both materials. Test cases are summarized in Table III. To evaluate the sensitivity of the model to temperature, particle hardness and shape, target values were sampled over a small range (the minimum value was set at 5% below the target value, and the maximum value was set at 5% above the target value). A particle hardness of 255 Hv represents a mineral that is harder than gypsum but softer than fluorite; silica sand generally has a hardness of 1100 Hv. The SPQs of 0.023 and 0.19 represent quantified particle shapes for glass beads and silica sand as reported by Stachowiak (2000).

Table III. Test Cases

Austenitic Stainless Steel	Units	Case 1	Case 2	Case 3	Case 4	Case 5	Case 6	Case 7	Case 8
Temperature	°C	65.6	65.6	65.6	65.6	93.3	93.3	93.3	93.3
Particle hardness	Hv	1100	1100	255	255	1100	1100	255	255
SPQ	-	0.023	0.192	0.023	0.192	0.023	0.192	0.023	0.192
Nickel Alloy	Units	Case 9	Case 10	Case 11	Case 12	Case 13	Case 14	Case 15	Case 16
Temperature	°C	65.6	65.6	65.6	65.6	93.3	93.3	93.3	93.3
Particle hardness	Hv	1100	1100	255	255	1100	1100	255	255
SPQ	-	0.023	0.192	0.023	0.192	0.023	0.192	0.023	0.192

Input values for other parameters in the erosion-corrosion model used in the sensitivity studies are provided below in Table IV.

Table IV. Additional Test Case Parameter Values

Parameter	Units	Minimum	Average	Maximum
Wear Allowance	m	-	2.4E-03	-
Velocity	m/s	2.5	3	3.7
Wt% Solids	-	2%	15%	27%
Mean Particle Size	micron	51.3	54	56.7
pH	-	12	14	15

ANALYSIS

Erosion-corrosion is a complex material degradation mechanism involving mechanical erosion and electrochemical corrosion. Results show that increasing spikiness (SPQ) of particle shape increases the total loss and probability of exceeding the wear allowance (best-estimate at 40 years). Likewise, increasing the temperature also increases the probability of exceeding the wear allowance and the average wear rate. Furthermore, decreasing particle hardness decreases the total loss and therefore probability of exceeding the wear allowance (best-estimate at 40 years). Results are summarized in Table V. Results indicate that harder materials are not necessarily more wear resistant [Lopez et al. 2005, and Rajahram et al. 2009]. Results also show that even though nickel alloys are marginally harder than stainless steels (resulting in a lower hardness factor compared to stainless steel hardness factor), nickel alloys have a higher temperature factor than stainless steels because of their lower melting temperature. The combined effect of hardness and temperature factors indicate that nickel alloys are less wear resistant than stainless steels.

Table V. Model Sensitivity Study Results

-	Case 1	Case 2	Case 3	Case 4	Case 5	Case 6	Case 7	Case 8
Average wear rate (mps)	2.1E-12	3.3E-12	5.27E-14	8.1E-13	2.2E-12	3.5E-12	5.85E-14	8.8E-13
40-YR Probability of Exceeding Wear Allowance	6.85E-01	9.95E-01	< 1.0 E-06	9.35E-06	7.89E-01	9.98E-01	< 1.0 E-06	3.33E-05
-	Case 9	Case 10	Case 11	Case 12	Case 13	Case 14	Case 15	Case 16
Average wear rate (mps)	2.28E-12	3.6E-12	5.56E-14	8.7E-13	2.4E-12	3.7E-12	5.86E-14	9.2E-13
40-YR Probability of Exceeding Wear Allowance	8.04E-01	9.98E-01	< 1.0 E-06	6.28E-05	8.66E-01	9.99E-01	< 1.0 E-06	1.89E-04

CONCLUSION

Erosion is an abrasive wear process caused by solid particle impacts on the surface. Corrosion is an electrochemical action of anodic dissolution of metal surfaces. Erosion-corrosion occurs when erosion and corrosion coexist. Erosion-corrosion models have been developed to better understand the significance of two parameters: relative hardness of the abrasive to the metal and the temperature. Relative hardness effects and temperature on total erosion-corrosion loss have been investigated independently, and this paper examines their combined effect on the target material.

Probabilistic calculations were performed to quantify the combined effect of relative hardness and temperature on liquid-particle induced erosion-corrosion using a model recently developed to predict pipe wall thinning. Calculations for average wear rates over 40 years were performed for stainless steel and nickel alloy materials exposed to different particle hardness and particle shapes, and temperatures. The probabilities of exceeding a predefined wear allowance indicate that harder target materials are not necessarily more wear resistant. Material selection should consider both corrosive and mechanical stressors to minimize total wear associated with erosion-corrosion. Erosion-corrosion probabilistic calculations will support the safe, efficient, and reliable operation of processing components over the design life.

REFERENCES

1. K. Chawla, K. Singh, N. Saini, and J. Singh. "Erosion Wear Behaviour of Chromium Coated Steel 304 and Grey Cast Iron," *International Journal of Innovative Research in Science, Engineering and Technology*, Vol. 2, Issue 9 (2013).
2. R.A. Flinn and P.K. Trojan, *Engineering Materials and Their Applications*, Fourth Edition, pp.113-116, John Wiley & Sons, Inc., United States of America (1995).
3. *ASM Handbook*, Volume 18, "Friction, Lubrication, and Wear Technology," ASM International, Materials Park, OH, U.S.A. (2003).
4. *Friction, Wear, and Wear Protection*, Edited by A. Fischer and K. Bobzin, Wiley-VCH& Co. KGaA, Germany (2009).
5. H.McI., Clark and R.J. Llewellyn, "Assessment of the Erosion Resistance of Steels Used for Slurry Handling and Transport in Mineral Processing Applications," *Wear* 250 (2001).
6. G.R. Desale, B.K. Gandhi, and S.C. Jain, "Slurry Erosion of Ductile Materials Under Normal Impact Condition," *Wear* 264 (2008).
7. G.W. Stachowiak, "Particle angularity and Its Relationship to Abrasive and Erosive Wear," *Wear* 241 (2000).

WM2016 Conference, March 6 – 10, 2016, Phoenix, Arizona, USA

8. Bahadur, S. and R. Badruddin, "Erodent Particle Characterization and the Effect of Particle Size and Shape on Erosion," *Wear*, 138 (1990).
9. S.A.M. Refaey, F. Taha, and A.M. Abd El-Malak, "Corrosion and Inhibition of 316L Stainless Steel in Neutral Medium by 2-Mercaptobenzimidazole," *International Journal of Electrochemical Science*, Vol.1 (2006).
10. M.R. Duignan, and S.Y. Lee. 2001. "RPP-WTP Slurry Wear Evaluation: Literature Review," WSRC-TR-2001-00156, Westinghouse Savannah River Company, Aiken, SC 29808.
11. N. Gat, and W. Tabakoff, "Effects of Temperature on the Behavior of Metals Under Erosion by Particulate Matter," *Journal of Testing and Evaluation (JTEVA)* Vol. 8, No. 4 (1980).
12. D. Lopez, J.P. Congote, J.R. Cano, A. Toro, and A.P. Tschiptschin. "Effect of Particle Velocity and Impact Angle on the Corrosion-Erosion of AISI 304 and AISI 420 Stainless Steels," *Wear*, 259 (2005).
13. S.S. Rajahram, S.S., T.J. Harvey, and R.J.K, Wood. "Erosion-Corrosion Resistance of Engineering Materials in Various Test Conditions," *Wear* 267 (2009).